BUTTERWORTH HEINEMANN

Polymer Vol. 36 No. 26, pp. 4899–4909, 1995

0032-3861/95/$10.00 + 0.00

polymer papers

Properties of chlorinated polyethylene waxes/poly(methyl methacrylate) blends: dependence of surface composition on wax chlorine content and blend composition

Dariusz M. Bielinski
Polymer Institute, Technical University of Lodz, Zwirki 36, 90-924 Lodz, Poland

and Stanley Affrossman*, Mark Hartshorne and Richard A. Pethrick
Department of Pure and Applied Chemistry, University of Strathclyde, 295 Cathedral Street, Glasgow G1 1XL, UK
(Received 7 October 1994; revised 20 February 1995)

Chlorinated polyethylene wax/poly(methyl methacrylate) (CPE/PMMA) blends have been investigated using X-ray photoelectron spectroscopy, static secondary-ion mass spectroscopy and contact angle measurements, and the surface composition has been observed to depend on the chlorine content in the wax and on the blend composition. Dielectric thermal analysis and dynamic mechanical thermal analysis measurements have been used to probe the phase structure of the blends and identify the glass transition temperature. These systems exhibit a complex phase behaviour with a microheterogeneous morphology. The waxes can be divided into two groups, according to their chlorination level: Cl $\leqslant$ 48 wt% and Cl > 48 wt%. The extent of specific interactions in the systems, determined using nuclear magnetic resonance and Fourier-transform infra-red spectroscopies, explains the differences in behaviour. A degree of chlorination >48 wt% is shown to be necessary for the CPE wax to form a sufficient number of hydrogen bonds to maximize compatibility with PMMA.

(Keywords: CPE/PMMA blends; miscibility; specific interactions)

INTRODUCTION

Poly(vinyl chloride)/poly(methyl methacrylate) (PVC/PMMA) blends have been investigated extensively because of their potential industrial usefulness[1]. Fewer studies have been devoted to the chemically similar chlorinated polyethylene (CPE) wax/PMMA[2–4] system. These blends deserve more detailed attention because the chloroparaffins are recommended plasticizers for PVC.

Miscibility between polymer materials is generally thermodynamically unfavourable and most systems show at best a microheterogeneous morphology[5]. The entropy of mixing for long molecules is small, in which case the enthalpy plays a dominant role in the Gibbs free energy of mixing. Specific intermolecular interactions, which are not present in the individual polymers but are present in the mixtures, can provide sufficient free energy to achieve a homogeneous morphology at a molecular level[1]. The free energy of mixing consists of three main contributions: the combinatorial entropy of mixing, the exchange interaction and the free-volume contribution, all of which are very small for high-molecular-mass components. The phase behaviour is the result of a very delicate balance between these contributions. For blends of a polymer with a small molecule, e.g. a plasticizer, the combinatorial entropy contribution will be significant.

Walsh *et al.*[2,3], Clark *et al.*[4], Vorenkamp and Challa[6] and Lemieux *et al.*[7] observed an effect of chlorination level of CPE, PVC or chlorinated PVC (CPVC) on the morphology of blends with PMMA. In spite of the range of different techniques utilized, they came to similar conclusions. It was found that CPE, PVC or CPVC containing 50–63 wt% of chlorine are compatible with PMMA. At lower or higher degrees of chlorination, the polymers were not compatible.

Miscibility in blends of CPE or PVC with PMMA may be attributed to specific attractive interactions between the carbonyl oxygens of PMMA and the α-hydrogens of CPE or PVC. However, dipole–dipole interactions between the carbonyl bond of PMMA and the carbon–chlorine bond of chlorinated polymers or hydrogen bonding involving the β-hydrogens of CPE or PVC cannot be excluded[8]. It has been proposed that the heat of mixing is unfavourable for chlorine contents up to 43 wt%, but at 52.9 wt% becomes favourable for compatibility[2,3]. Compatibility leads to the generation of clear films, but the formation of heterogeneous films can depend on the way in which the blends are produced. An increase in the chlorine content of CPE results in a decrease of the temperature of phase separation, which in turn increases with an increase in the syndiotactic

* To whom correspondence should be addressed

structure of PMMA[7,9,11]. Quantitative comparison of data from different laboratories is difficult, because different samples have been used. The variation of parameters such as the level of chlorination in CPE/PVC, the tacticity of PMMA, the molecular weights of the individual components, the conditions used in preparation of the blends, and the range of experimental techniques applied for investigation of the blends, all influence the results obtained.

This study examines the relationship between the bulk and surface structure of the CPE wax/PMMA blends. The molecular structures of the CPE waxes and PMMA are estimated from ^{1}H and ^{13}C nuclear magnetic resonance (n.m.r.), and the strengths of specific interactions occurring in the blends are assessed by spectral shifts observed in Fourier-transform infra-red (*FT*i.r.) spectra. The paper reports the use of dielectric thermal analysis (d.e.t.a.) and dynamic mechanical thermal analysis (d.m.t.a.) to explore the phase behaviour. The surface structure is determined using X-ray photoelectron spectroscopy (X.p.s.), static secondary-ion mass spectroscopy (s.s.i.m.s.) and contact angle measurements.

EXPERIMENTAL

Materials and their characterization

The materials examined are listed together with their physical properties in *Table 1*. Commercial-grade chloroparaffins were purified by vacuum distillation into a cold trap. Mass spectroscopy did not reveal any traces of antioxidants in the materials. The polymer molecular weight and distribution were characterized by gel permeation chromatography (g.p.c.) using a Waters chromatograph with μ-Styragel columns. Polystyrene was used as a calibration standard and the measurements were conducted at room temperature in tetrahydrofuran for PMMA and chloroform for CPE waxes. Mark-Houwink paramaters for polystyrene were used to process the data for CPE waxes, because the parameters for chloroparaffins are not available. The 'molecular weights' obtained were only used as a check on the relative size of the waxes.

The densities of the samples (*Table 1*) were measured using a pycnometer.

The glass transition temperature was determined using a DuPont 910 Differential Scanning Calorimeter, equipped with a 9200 microcomputer. Scans were performed at a heating rate of 10 K min^{-1} over the temperature range 213–293 K. Elemental chemical microanalysis data are presented in *Table 1*.

Blend preparation

Blends were prepared in two different ways. Samples for d.e.t.a. and d.m.t.a. were cast directly from 8 wt% solution in toluene (Analar) onto copper electrodes (d.e.t.a.) or brass foil (d.m.t.a.). Solvent evaporation was carried out at room temperature and the samples, once they had passed the tacky stage, were stored in a vacuum oven at 298 K until they reached constant weight. Samples for X.p.s., s.s.i.m.s., contact angle measurements and *FT*i.r. were spun, using a spinner (Headway Research Inc., USA), from 4 wt% solution in toluene (Analar) onto silicon wafers, or onto KBr discs for *FT*i.r. The thickness of the films was measured using a Dektak IIA instrument (RPI Metrolog Division, UK), and was determined to be between 0.2 and 0.4 μm for spun and between 40 and 60 μm for cast films respectively. Recent studies[12] would imply that these films should have similar properties, although it can be argued that differences may be expected.

Compositions are expressed in weight percentage or monomer percentage. The average monomer structure of the wax ($-C_2H_{4-x}Cl_x-$) was considered, where x values were calculated from chemical microanalysis. For example, the monomer composition of S50 5 wt%/PMMA blend is as follows:

microanalysis of the wax (wt%)

C = 42.92, H = 6.21, Cl = 50.63 $\Rightarrow x = 0.78$

wax monomer percentage = 8.7,

PMMA monomer percentage = 91.3

Techniques

Nuclear magnetic resonance. Samples were investigated using either a 250 MHz or 400 MHz Bruker *FT* n.m.r. instrument, for ^{1}H or ^{13}C experiments respectively. Spectra were obtained over the range 0–7.5 ppm in the case of ^{1}H, and 0–200 ppm for ^{13}C n.m.r. Proton decoupling was applied to resolve the spectra. The

Table 1 Physical properties of polymers investigated

No.	Sample[a],	Molecular weight[b] $\bar{M}_w$ CHCl	THF	$\bar{M}_w/\bar{M}_n$ $CHCl_3$	THF	Density[c], ρ (g cm^{-3})	Glass transition temp.[d], T_g (K)	Chemical microanalysis (wt%) C	H	Cl	Pour point, T_p (K)
1	PMMA	233500	210600	2.1	2.0	1.1882	382.9				453.3[e]
2	S42	98.5	408.3	1.6	1.1	1.1604	222.7	49.41	7.40	43.16	243.3
3	S48	122.7	1373.0	1.8	1.2	1.2432	242.2	43.70	6.32	49.49	258.3
4	S50	46.1	148.6	2.2	1.6	1.2494	222.4	42.92	6.21	50.63	264.3
5	S58	68.6	271.2	1.5	1.2	1.3628	259.5	36.30	4.55	58.70	280.3

[a] ICI Chloro-Chemicals, Cereclor
[b] Calculated from g.p.c. measurements (in polystyrene equivalents)
[c] Determined pycnometrically
[d] Obtained from d.s.c. experiments
[e] Aldrich, melting point, T_g = 387 K

samples were measured in a solution in d-toluene with a tetramethylsilane (TMS) reference.

Fourier-transform infra-red spectroscopy. Samples were analysed using a Mattson 5000 (Unicam Analytical Systems, UK) *FT* i.r. instrument over the wavelength range 600–2000 cm^{-1}, in two different regimes: first, using 128 scans at 2 cm^{-1} for initial examination of CPE waxes or CPE wax/PMMA blends at different compositions, and secondly using 1000 scans at 0.75 cm^{-1} for spectral shift determination.

Dielectric thermal analysis. The films were dried in a vacuum chamber at 298 K for 72 h prior to being investigated. Dielectric thermal analysis (d.e.t.a.) experiments were performed over a frequency range 10^{-1}–10^{5} Hz and a temperature range 203–383 K, using a computer-controlled frequency response analyser with a charge amplifier. The system has been described in detail elsewhere[13]. Data obtained from the apparatus were processed to yield the dielectric constant (E') and loss (E'').

Dynamic mechanical thermal analysis. The PL-DMTA III dynamic mechanical thermal analyser (Polymer Laboratories Ltd, UK) was used in the single-bending-mode configuration. Films on a thin brass foil (thickness = 0.14 mm) were subjected to imposed oscillatory frequencies of 1 and 10 Hz. A temperature range 203–393 K was scanned at 2 K min^{-1} heating rate. Loss tangent curves were analysed by subtraction of the response of the foil background. A maximum in the tan δ curve was taken as an indication of the glass transition region of the blends.

X-ray photoelectron spectroscopy. Samples were irradiated by a Vacuum Science Workshop X-ray anode, operating at 110–130 W of power, and generating Al Kα photons (1486.6 eV). The Vacuum Science Workshop 100 mm Concentric Hemispherical Analyser was operated in the FAT (fixed analyser transmission) mode with a 50 eV pass energy, and the electron take-off angle was normal to the surface.

Relative atomic concentrations of C, O and Cl present on the surface were calculated using Wagner's sensitivity factors[14], modified for our instrument.

The monomer fraction of wax on the surface was taken as:

$$\text{wax monomer percentage} = \frac{Cl}{Cl + (x/2)O} \times 100$$

where x = the number of chlorine atoms present in an 'average' (PVC) CPE wax monomer unit, calculated from the chemical microanalysis, i.e. ($-C_2H_{4-x}Cl_x-$), and Cl, O = the atomic contents of chlorine and oxygen respectively, calculated from the X.p.s. data.

Static secondary-ion mass spectroscopy. Samples were irradiated with a Vacuum Science Workshop ion gun, using a 3 keV argon-ion beam. A current of 0.2 nA, measured at the ion gun, was focused on an area of ca. 5 mm^2 at the sample. A flood gun used to compensate charging was set to 30 eV. Upon emission, the secondary particles passed through an Einzel Lens Energy Filter, designed in-house, which focused the ions. Mass discrimination was obtained with a Vacuum Generators 12–12 quadrupole.

Positive spectra were found to be uninformative, owing to the variety of ion fragmentation processes taking place. The negative spectra were more readily interpreted. The heights of the peaks observed at m/e 16, 25 and 35, coming from O, C_2H and Cl respectively, were determined. The contribution of the higher-mass chlorine-containing fragments was ignored, because of the small size of the signals detected.

The height of the peak coming from O, I_{16}, was compared to the height of the peak originating from Cl, I_{35}, using the C_2H peak, I_{25}, as a reference, because the data were obtained in two mass ranges m/e 15–27 and 24–36.

The monomer fraction of wax on the surface was taken as:

$$\text{wax monomer percentage} = \frac{I_{35}}{I_{35} + yI_{16}} \times 100$$

where y = the relative s.s.i.m.s. sensitivity factor, calculated from the X.p.s. measurements of compatible mixtures (S50 or S58/PMMA blends containing <5 wt% of the wax):

$$\text{wax monomer percentage (X.p.s.)} = \frac{I_{35}}{I_{35} + yI_{16}} \times 100$$

The average y value calculated for 3 and 5 wt% of the wax was used for the data calculation of all systems.

Contact angle measurements. Contact angles were determined with a Contact Master CMC instrument (Interskill Ltd, UK), equipped with a goniometer. Two liquids with extremely different polarities[15] were used, distilled water and diiodomethane (methylene iodide). The surface energy (γ_S) for water is 72.6×10^{-3} J m^{-2} with $\gamma_S^d = 21.6 \times 10^{-3}$ and $\gamma_S^p = 51.0 \times 10^{-3}$, and for diiodomethane is 50.8×10^{-3} J m^{-2} with $\gamma_S^d = 48.5 \times 10^{-3}$ and $\gamma_S^p = 2.3 \times 10^{-3}$ (ref. 15), where γ_S^d and γ_S^p are respectively the dispersion and polar components of the total surface energy. Neither of the liquids induced swelling of the polymers. The experiments were carried out under ambient conditions and the surface energy was calculated from the contact angle values, according to the procedure described by Janczuk and Bialopiotrowicz[16]. The polar interaction parameter was taken as a geometric mean of the polar components, as suggested in the literature[16–18].

RESULTS AND DISCUSSION

Molecular structure

Nuclear magnetic resonance spectroscopy. Miscibility in blends of the polymers studied has been ascribed to a specific attractive interaction between the acidic hydrogen of CPE or PVC and the basic oxygen from the carbonyl group of PMMA. The interaction is generally thought to be the result of either hydrogen bonding[9,19,20] or a Lewis acid–base interaction[8,21,22].

N.m.r. spectroscopy was used to establish the structure of the materials. ^1H n.m.r. experiments were performed for PMMA, to determine its configuration, because there is some evidence that tacticity can influence

Table 2 PMMA structure, worked out from ^{1}H n.m.r. experiment

	Diad analysis[a]			Triad analysis[c]			Number-average block length		
Material	r	m	σ^b	i	a	s	n_i	n_s	$\bar{n}^d$
PMMA	0.88	0.12	0.12	0.04	0.45	0.52	1.14	8.40	4.76

[a] Diad analysis performed according to the procedure described by White and Flisko[24]
[b] Probability that a polymer chain will add a monomer unit to give the same configuration as that of the last unit at its growing end
[c] Triad analysis performed according to the procedure described by Bovey and Tiers[25]
[d] Number-average length of a repeat unit

Table 3 Possible three-carbon sequences in CPE waxes[27] (0 equates with CH_2; 1 with CHCl; and 2 with CCl_2)

CH_2-centred	CHCl-centred	CCl_2-centred
$\{000\}^{a,b,c,d}$	$\{010\}^{a,b,c,d}$	$\{020\}^{c,d}$
$\{001\}^{a,b,c,d}$	$\{110\}^{a,b,c,d}$	$\{120\}^{d}$
$\{002\}^{c}$	$\{111\}^{a,b,c,d}$	$\{121\}^{a,b,c,d}$
$\{101\}^{a,b,c,d}$	$\{210\}^{c}$	$\{220\}^{c}$
$\{201\}^{a,b,c,d}$	$\{211\}^{d}$	$\{221\}^{c}$
$\{202\}^{c}$	$\{212\}^{c}$	$\{222\}^{c}$

Peaks in the spectra were assigned according to Zhou *et al.*[26] and Komoroshi *et al.*[27]. The sequences observed are designated as: [a] for S42, [b] for S48, [c] for S50, [d] for S58, and [e] not observed

compatibility with chlorinated polymers[9-11,23]. An increase of the extent of random structure in the chains leads to a corresponding increase in blend miscibility. Analysis of the ^{1}H n.m.r. spectra was performed according to the procedure described earlier by White and Flisko[24] and Bovey and Tiers[25]. The results (*Table 2*) indicate that the structure is not random. The tactic content of PMMA from a triad analysis, i.e. isotactic : atactic : syndiotactic (i : a : s) segments, differs significantly from the 1 : 2 : 1 ratio characteristic for random PMMA.

N.m.r. experiments were also carried out for the chlorinated waxes. Interpretation of the ^{13}C n.m.r. spectra was performed according to Zhou *et al.*[26] and Komoroski *et al.*[27,28]. The general structure of CPE wax was assumed, following Keller[29,30], to be of the ethylene–vinyl chloride copolymer type, for which the 1,2-dichloroethane fragment is characteristic. Such a structure was reported to be adequate for CPE waxes with a low or medium degree of chlorination, smaller than the 57 wt% characteristic of PVC. A signal from dichlorinated methylene, corresponding to a vinylidene chloride unit (chemical shift of $-CCl_2-$ larger than 90 ppm[30,31]), is visible in spectra of all the waxes. Its magnitude is, however, very small, even in the case of higher-chlorine-content chloroparaffins, being practically absent for S42 wax. ^{13}C n.m.r. spectra of S58 or S50 waxes contain two small peaks in the $-CCl_2-$ region (90–100 ppm), whereas in the case of S48 and S42 chloroparaffins only one peak could be resolved. The possible three-carbon sequences in the waxes are shown in *Table 3*[27].

CPE waxes have a random structure, contrary to chlorinated PVC (CPVC). Such a structure is less prone to crystallization[32]. The degree of chlorination, calculated from the n.m.r. spectra, is in good agreement with that obtained from chemical microanalysis. From structural data (*Table 4*) the susceptibility of the CPE waxes to specific interactions, indicated by the ratio of CH/CH_2 groups, can be calculated. We suggest that chlorination increases the number of the $-CHCl-$ groups that are involved in specific interactions, thus improving miscibility. At lower chlorination levels, below 50 wt%, the number of $-CH_2-$ groups becomes significant, decreasing the intermolecular interactions.

Values of CPE wax 'acidity', CH/CH_2, shown in *Table 4*, confirm a connection between the chlorine content and the potential for specific interaction of the waxes. The ratio of about 0.4 calculated for S48 seems to be a boundary value, above which a critical number of interactions can occur. In the spectra of the blends, however, no shift was observed of the carbonyl group frequency from the pure PMMA, indicating interaction with the acidic hydrogen from CPE wax to be transient and weak.

Fourier-transform infra-red spectroscopy. The potential for formation of the specific interactions in chlorinated polyethylene wax blends with PMMA was also investigated by *FT* i.r. spectroscopy. The data are presented in *Table 5*. An increase in the ratio of CH/CH_2 groups due to the changes in the chlorine content of the wax confirms the n.m.r. results presented above.

To determine the relative magnitude of the effect of specific interactions, mixtures of the waxes with pyridine, which is a stronger base than PMMA, were analysed. For pyridine, the bands of interest for hydrogen bonding correspond to stretching vibrations of heterocyclic double bonds at 1550–1600 cm^{-1} (ref. 33) (an intense vibration at 1597 cm^{-1} and a weaker one at 1558 cm^{-1}) and C=N vibrations at 1581 cm^{-1} (ref. 34). Changes in the band intensity ratios of 1581 cm^{-1}/1597 cm^{-1} (*Table 5*) for a 50 : 50 weight composition of the waxes with pyridine indicate an involvement of pyridine nitrogen in specific interactions with the *a*-hydrogen from the wax. An increase in the ratio with increase of the chlorine content in CPE waxes indicates a higher number of specific interactions.

Table 4 CPE wax compositions, evaluated from ^{13}C n.m.r. spectra

		Chlorine content (wt%)		Composition[a] (mol%)				
No.	Sample	Microanalysis	N.m.r.	CH_2	CHCl	CHCl–CHCl	CCl_2	CH/CH_2
1	S42	43.16	43.24	74.9	19.0	6.1	0.0	0.34
2	S48	49.49	49.01	70.9	17.2	11.3	0.6	0.40
3	S50	50.63	51.01	68.5	18.5	11.5	1.5	0.44
4	S58	58.70	59.55	52.4	31.6	13.5	2.5	0.86

[a] Sequence composition was evaluated according to Zhou *et al.*[26] and Komoroski *et al.*[27,28]

Table 5 *FT* i.r.data on the CPE waxes and their interactions with pyridine and with PMMA

No.	Sample[a]	Absorbance ratio[b] CH_2/CH_3 1453/1377	CH/CH_3 1263/1377	Cl/CH_3 659/1377	CH/CH_2 1263/1453
1	S42	2.97	2.06	1.84	0.70
2	S48	2.70	2.10	2.19	0.78
3	S50	2.85	2.45	2.36	0.87
4	S58	3.09	2.91	>4	0.94

No.	Sample	Absorbance ratio[b] CH/COOMe 987/1148	987/1241	CH/C=O 987/1731	CH_2/C=O 1442/1731	CH/CH_2 987/1442
1	S42/PMMA	0.11	0.28	0.02	0.06	0.35
2	S48/PMMA	0.12	0.29	0.02	0.06	0.40
3	S50/PMMA	0.12	0.30	0.02	0.05	0.43
4	S58/PMMA	0.18	0.45	0.03	0.05	0.64

No.	Sample	Specific interactions[b,c] 1581 cm^{-1}/1597 cm^{-1}
1	Pyridine	1.08
2	S42/pyridine	1.27
3	S48/pyridine	1.35
4	S50/pyridine	1.84
5	S58/pyridine	1.87

No.	Sample	Band shift[d] (cm^{-1})	ΔH_m[e] ($kJ\,mol^{-1}$)
1	S42/PMMA	0	0.484
2	S48/PMMA	0.96	−0.464
3	S50/PMMA	0.96	−0.613
4	S58/PMMA	1.92	−1.561

[a] ICI Chloro-Chemicals, Cereclor

[b] *FT* i.r. analysis has been carried out in the regime: 128 scans/2 cm^{-1} accuracy

[c] Pyridine band wavelengths have been assigned: 1581 cm^{-1} to C=N vibrations, and 1597 cm^{-1} to stretching vibrations of heterocyclic double bonds, according to Cesteros *et al.*[33] and Klinsberger[34]

[d] *FT* i.r. analysis has been carried out in the regime: 1000 scans/0.75 cm^{-1} accuracy

[e] Enthalpy of mixing (ΔH_m) values were calculated, taking into consideration the contribution of dispersion forces to the shift (worked out from the dispersion component of surface energy, γ_S^d), according to the procedure described by Fowkes *et al.*[22,35]. The shift of the carbonyl band of PMMA was found to be constant between wax concentrations from 5 wt% to the highest measured concentration of 25 wt%

Fourier-transform infra-red spectroscopy of blends. Only blends containing 5 wt% (≈7–11 monomer per cent for S58–S42 respectively) of wax were considered, this concentration being within the recommended range for the CPE plasticizers. *FT* i.r. experiments performed on CPE waxes/PMMA system (*Table 5*) are consistent with the results of n.m.r. studies.

The ratio of C–H stretching at 987 cm^{-1} to ester group vibrations at 1241 or 1148 cm^{-1}, taken as a reference, increases on addition of wax. The calculated values of CH/CH_2 ratios show the same tendency. The increase is dependent on chlorine content, being higher for the more chlorinated materials. On the other hand, the quantity of CH_2 groups, measured as the ratio of CH_2/C=O band intensities, goes down with increasing chlorine content in the CPE wax.

Some displacement of the bands, i.e. the C–H stretching at 987 cm^{-1} and the $(CH_2)_{n>3}$ at 720 cm^{-1}, towards higher wavelengths is observed. The former is not significant, a maximum of 3 cm^{-1}, and takes place only for systems containing waxes of medium or higher degrees of chlorination (>42 wt%). The latter, however, is more pronounced and visible in all cases. Ma and Prud'homme[37] have suggested that this is evidence for specific interactions between the β-hydrogen from the wax and the carbonyl oxygen from PMMA.

Other *FT* i.r. experiments on CPE wax/PMMA blends focused on shifts of the carbonyl band, and were directly connected with the strength of specific interactions. A shift towards lower wavelength values has been observed only in the case of systems containing waxes with high chlorine contents. From the band shift values the enthalpy change, ΔH_m, due to specific (hydrogen-bonding) interactions can be calculated, according to the empirical equation proposed by Fowkes *et al.*[22].

Considering the i.r. shifts ($\Delta\nu$) for interaction of PMMA with acidic materials, it is possible to obtain information on the nature of the acid.

The stretching frequency of bonded carbonyl oxygens is decreased by an amount ($\Delta\nu^m$) proportional to the enthalpy of bonding (ΔH_m)[22,35]:

$$\Delta\nu^m = (\Delta H_m)/0.99$$

where ΔH_m is in $kJ\,mol^{-1}$ and $\Delta\nu^m$ is in cm^{-1}.

The carbonyl shifts measured from the *FT* i.r. spectra, $\Delta\nu$, are first corrected for the dispersion force contribution, $\Delta\nu^d$:

$$\Delta\nu^m = \Delta\nu - \Delta\nu^d$$

Following Fowkes, $\Delta\nu^d$ is calculated from the experimental data[22] for the carbonyl stretch frequency of the PMMA complex, $\Delta\nu_{CO}$, as a function of the dispersion component of the surface energy, γ_S^d.

The value of $\Delta\nu^d$ for the CPE wax/PMMA system was very small (≈0.5 cm^{-1}), below the accuracy of the spectrometer.

The $|\Delta H_m|$ values obtained for the chloroparaffins studied (*Table 5*) are also small and of similar value to CH_2Cl_2 but appreciably lower than for $CHCl_3$ (ref. 22), which explains the sensitivity of the blends to environmental factors, such as trace amounts of water.

They are of the same order of magnitude as those reported by Chai *et al.*[3] and Vorenkamp and Challa[6] for mixtures of low-molar-mass analogues of PVC (1,3-dichlorobutane or chlorinated octadecanes respectively) and PMMA (methyl ester of isobutyric acid or oligomeric methacrylate respectively), ≈ −0.15 to +0.16 kJ mol^{-1}. The calculated values of the enthalpy of mixing (ΔH_m) for the system studied are higher, because in the case of CPE wax and PMMA, there are more active centres (α-H and C=O) present. Exothermic mixing was observed only for the blends containing waxes with chlorine content above 42 wt%. In the case of systems containing chloroparaffins S48 or S50, the ΔH_m values obtained are negative but small, and close to each other.

Bulk analysis

Differential scanning calorimetry. The glass transition temperatures, T_g, of the waxes, obtained from d.s.c. measurements, are given in *Table 1*. The value of T_g increases with chlorine content, and with molecular weight, as may be expected.

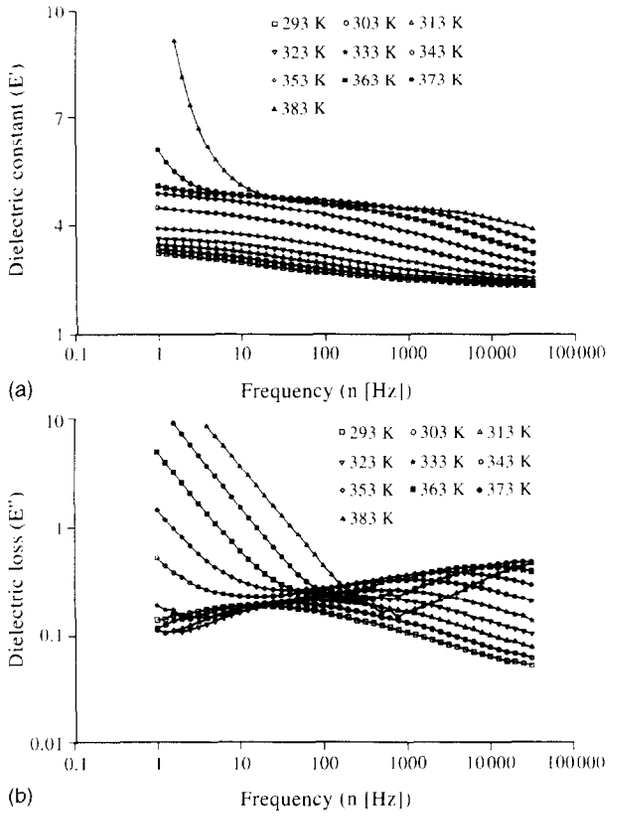

Figure 1 Changes in dielectric properties of PMMA with frequency, calculated from d.e.t.a.: (a) dielectric constant (E'), (b) dielectric loss (E'')

A considerable literature exists on chlorinated polymer/polyester systems[4,6,9–11,19–21,36–43]. Some of the measurements, e.g. d.s.c., which attract the most interest[21,40–43], are not very sensitive to small differences in polymer miscibility at a molecular level. The results obtained are very difficult to interpret, because there is an absence of well defined phase transition regions in the d.s.c. curves. However, a conclusion can be drawn concerning the microheterogeneity of the blends. According to Fried *et al.*[44] and Kaplan[45], the limit on the scale of observation using the d.s.c. method is probably of the order of 20–30 nm. It is likely that such a degree of sensitivity is not sufficient to investigate the extent of mixing of the two polymers. The work of Parmer *et al.*[21] or more recently of Sofue and Tamura[42] suggests that the upper limit to heterogeneity of PVC/PMMA blends is approximately 3 nm.

Prud'homme has more recently used other techniques for determination of compatibility of chlorinated polymer/polymethacrylate blends[40].

Another controversial technique, light scattering[7,10,40], in principle is a very useful method, but, owing to the small refractive-index difference between PMMA ($n = 1.495$) and CPE ($n = 1.540$), it is very difficult to determine the cloud-point curve correctly and unambiguously[46].

Dielectric thermal analysis. In these systems, d.e.t.a. could be used to study compatibility, since the chlorinated polyethylene waxes contain C–Cl permanent dipole groups. The experiments were, however, limited

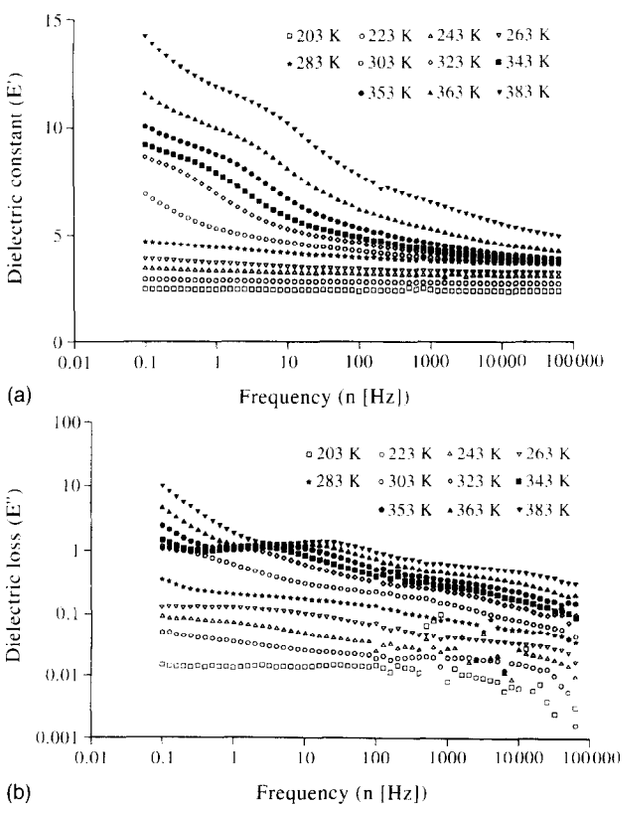

Figure 2 Changes in dielectric properties of S42/PMMA (5/95 wt%) blend with frequency, calculated from d.e.t.a.: (a) dielectric constant (E'), (b) dielectric loss (E'')

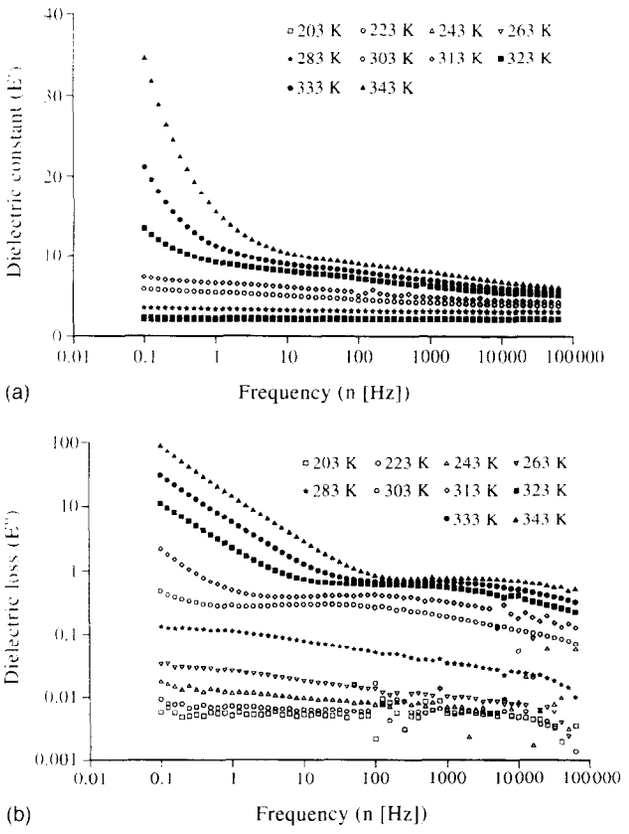

Figure 3 Changes in dielectric properties of S48/PMMA (5/95 wt%) blend with frequency, calculated from d.e.t.a.: (a) dielectric constant (E'), (b) dielectric loss (E'')

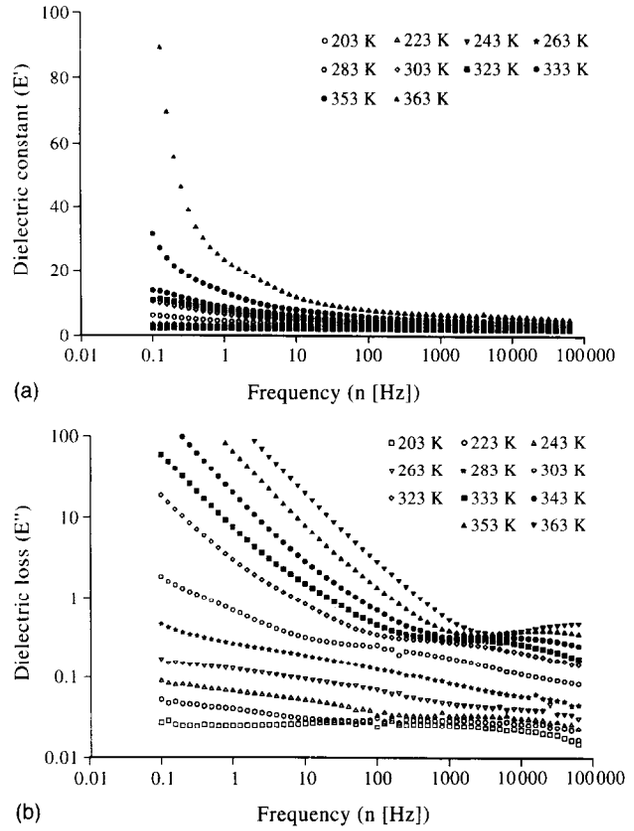

Figure 4 Changes in dielectric properties of S50/PMMA (5/95 wt%) blend with frequency, calculated from d.e.t.a.: (a) dielectric constant (E'), (b) dielectric loss (E'')

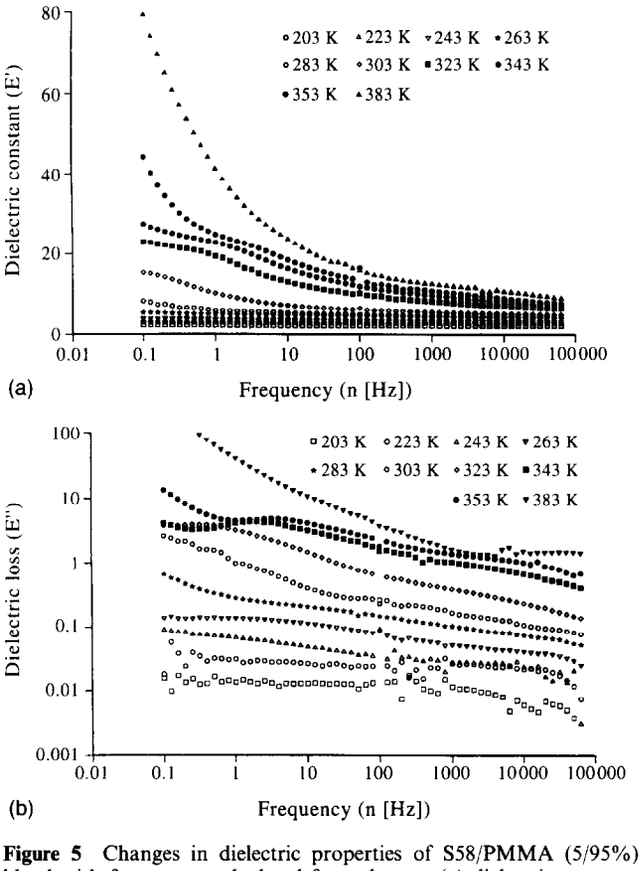

Figure 5 Changes in dielectric properties of S58/PMMA (5/95%) blend with frequency, calculated from d.e.t.a.: (a) dielectric constant (E'), (b) dielectric loss (E'')

because of decomposition of the wax component, which takes place at 333–343 K. Chlorine ions released during the decomposition process dramatically changed the conductivity of the sample and masked the dipolar relaxation process. In spite of this difficulty, it was still possible to observe the β transition of PMMA (T_β = 313–323 K) and the glass transition region of the chloroparaffins. Results of d.e.t.a. analysis are shown in *Figures 1–5*. Blends up to 5 wt% (≈7–11 monomer per cent for S58–S42 respectively) of wax were investigated. The β relaxation of PMMA is clearly visible in *Figure* 1. Significant increases of the dielectric constant (E') and dielectric loss (E''), occurring at higher temperatures ($T > 373$ K), are connected with the relaxation of the backbone of the polymer (α relaxation). *Figure 2* shows the occurrence of two relaxations in the case of S42/PMMA blend, indicating the coexistence of two phases. The beginning of the first is observed between 323 and 343 K; the second starts at 343 K. For S48 or S50/PMMA blends only one relaxation is observed, between 303 and 323 K (*Figures 3* and *4*). Because of the high values of dielectric constant E' obtained, it is likely that a single, microheterogeneous phase morphology prevails in these systems. Rather unexpectedly, phase separation is also observed when the highest-chlorine-content wax (S58) was blended with PMMA (*Figure 5*). The first relaxation process in this case starts between 303 and 323 K; the second begins at 323 K. Considering the E' data, microheterogeneity of the blend can also be concluded.

In all systems, high mobility of the PMMA main-chain groups was detected at higher temperatures. In spite of slight differences in the start temperature, from blend to blend, the initial point at about 323 K, or 353 K, can be observed for S48(S50)/PMMA or S42(S58)/PMMA blends, respectively.

The observation of the second relaxation requires some comments on the origin of possible processes in these systems. The low-molecular-mass CPE wax will exhibit a whole-molecule rotation, but is unlikely to exhibit a dipolar process in the frequency range studied. The extra relaxation can therefore be ascribed to the presence of a heterophase in the system. The generation of a separate phase will result in it behaving like a molar dipole with dimensions and relaxation characteristics controlled by the mobility of the molecular structure. Such features have been clearly seen in the systems, and are characteristic of the morphology of the materials. The process in this case is not resolvable from the more dominant dipolar relaxation and it is not possible to use the process to yield morphological data with any certainty. However, it is clear that the duration of this additional process is consistent with the microheterogeneous structure of the films.

Dynamic mechanical thermal analysis. According to theory, the data from d.e.t.a. and d.m.t.a. experiments should be related, certainly in a qualitative, if not always in a quantitative, way. The results of d.m.t.a. measurements are shown in *Figures 6–9*. The minor fluctuations near 273 K are artefacts, caused by a small amount of ice melting on the probe. The dominant structures at higher temperature indicate incompatibility to some extent in all blends being investigated. The glass transition peak is complex for all mixtures, but its form varies from sys-

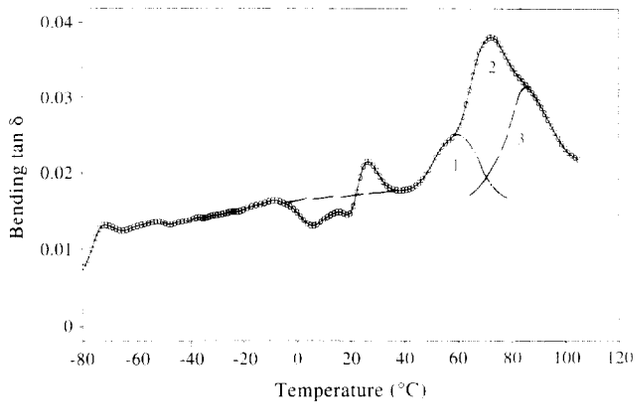

Figure 6 Changes in loss tangent (tan δ) of S42/PMMA (5/95 wt%) blend with temperature, obtained from d.m.t.a.: frequency $f = 1$ kHz; $dT/dt = 2\,K\,min^{-1}$. 1, 2, 3—see text

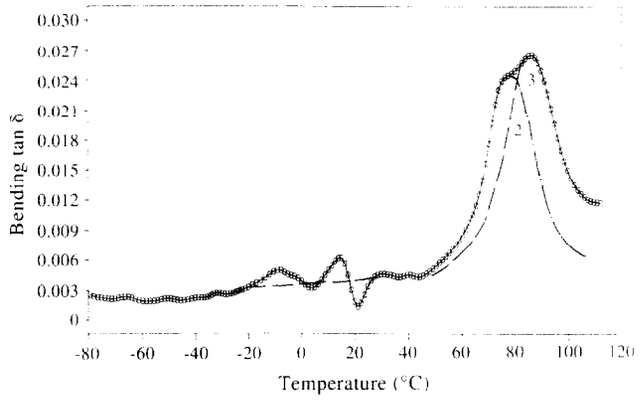

Figure 7 Changes in loss tangent (tan δ) of S48/PMMA (5/95 wt%) blend with temperature, obtained from d.m.t.a.: frequency $f = 1$ kHz; $dT/dt = 2\,K\,min^{-1}$

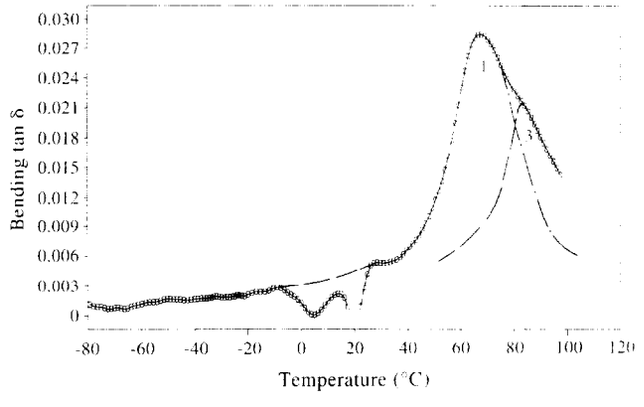

Figure 8 Changes in loss tangent (tan δ) of S50/PMMA (5/95 wt%) blend with temperature, obtained from d.m.t.a.: frequency $f = 1$ kHz; $dT/dt = 2\,K\,min^{-1}$

tem to system. In the case of the S42/PMMA blend three contributions can be distinguished (*Figure 6*), whereas for the other pairs only two are seen. Their positions can be roughly estimated as follows: 1. 330 K, 2. 350 K and 3. 360 K. The second and third peaks dominate the spectra of the S42(S48)/PMMA blends (*Figures 6* and *7*), whereas the first and third peaks are characteristic of S50(S58)/PMMA systems (*Figures 8* and *9*). These results indicate the most complex phase structure in the

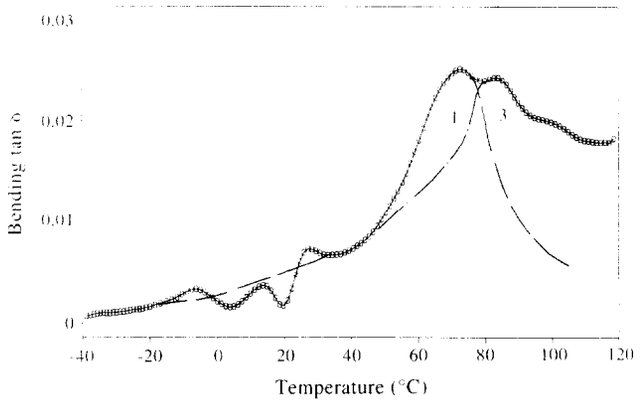

Figure 9 Changes in loss tangent (tan δ) of S58/PMMA (5/95 wt%) blend with temperature, obtained from d.m.t.a.: frequency $f = 1$ kHz; $dT/dt = 2\,K\,min^{-1}$

case of the blends prepared with the wax of lowest chlorine content. The data suggest heterogeneous structures of the blends, being in good agreement with the d.e.t.a. results. However, they additionally allow two groups of phase behaviour to be distinguished, namely: low-chlorine-content waxes (Cl < 48 wt%)/PMMA, and higher-chlorine-content waxes (Cl > 48 wt%)/PMMA blends.

The position of peak 1, dominating the d.m.t.a. spectra of S50(S58)/PMMA systems, at about 330 K, is in reasonable agreement with the theoretical T_g value for a fully compatible system ($T_g \approx 325$ K), calculated from the Fox equation[47]. The absence or small contribution (S42) of this peak to the overall glass transition indicates the immiscibility of the low-chlorine-content waxes with PMMA.

D.m.t.a. results are consistent with these coming from d.e.t.a. experiments. The observation of a single relaxation in dielectric measurements in the case of S48(S50)/PMMA blends may be explained as a result of the close proximity of the second process. However, at the lower frequencies used in d.m.t.a. these processes are resolved.

Surface analysis

Solution-cast blends of PMMA with chlorinated polyethylene waxes were found to produce clear films over a wide range of chlorine content (42–58 wt%), implying homogeneous or microheterogeneous mixing of the components. Surface analysis data revealed that, even if the bulk is homogeneous, the surface composition may differ from the bulk value because of the surface energy differences of the components.

The blends containing up to ≈10 monomer per cent (4–7 wt% for S42–S58 respectively) of the wax were of most concern, because of their known application, but data above this concentration, up to ≈40 monomer per cent (18–26 wt% depending on the wax) are also shown.

X-ray photoelectron spectroscopy. Results obtained from X.p.s. investigations are shown in *Figure 10* as a wax excess quantity (concentration observed – bulk concentration).

CPE wax/PMMA blends were found to have a slight surface enrichment or a depletion of the chlorinated wax, depending on the chlorine content and the blend composition.

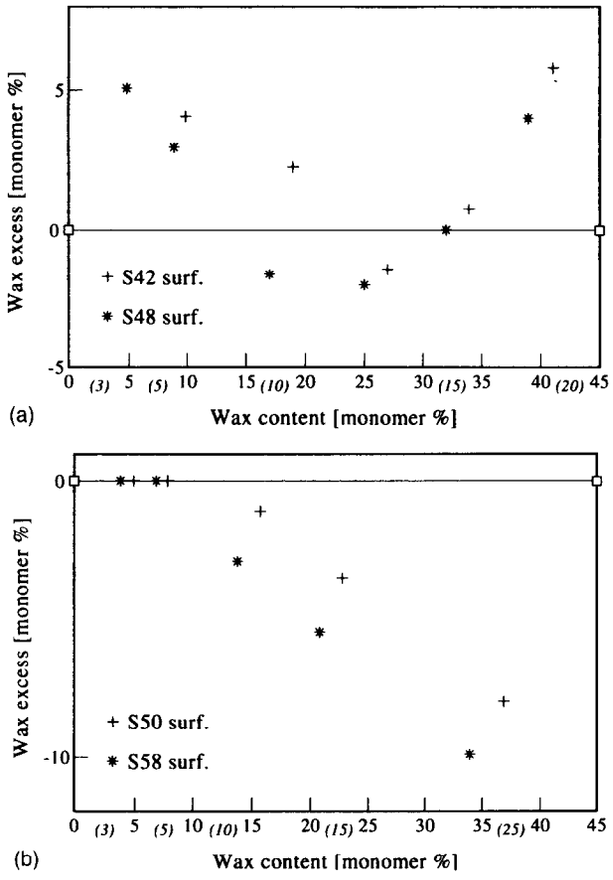

Figure 10 Surface CPE wax/PMMA composition in comparison to the bulk one, determined from X.p.s.: (a) S42 and S48; (b) S50 and S58. CPE wax content (wt%) is given in brackets

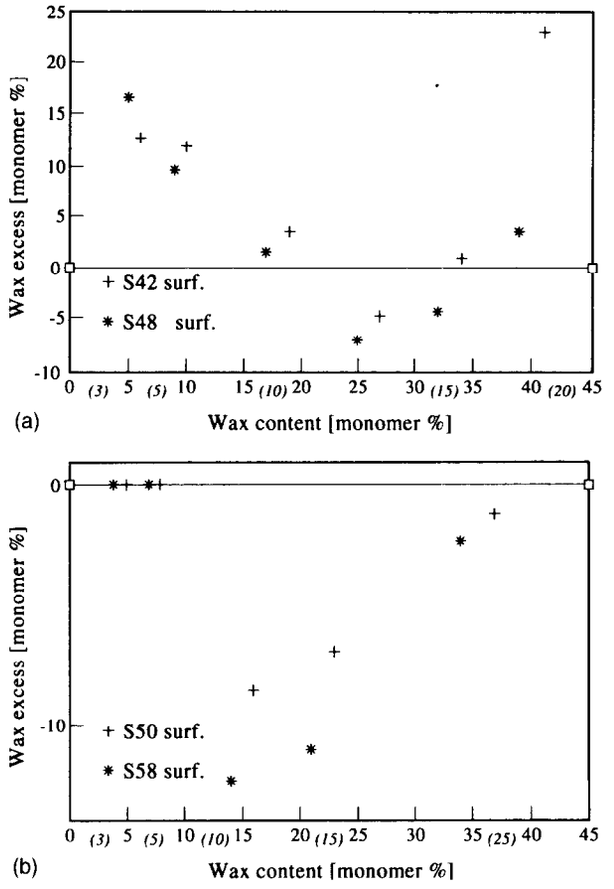

Figure 11 Surface CPE wax/PMMA blend composition determined from s.s.i.m.s.: (a) S42 and S48; (b) S50 and S58. CPE wax content (wt%) is given in brackets

Low-chlorine-content waxes (Cl $\leqslant$ 48 wt%) exhibit a segregation of the wax to the surface at low wax contents (*Figure 10a*). The surface excess of wax goes through a minimum, reaching a slightly negative value, as the wax content increases, and then returns to a positive excess at higher wax concentrations.

High-chlorine-content waxes (Cl > 48 wt%) have identical surface and bulk compositions up to $\approx$8–9 monomer per cent for S58 and S50 respectively (5 wt%) of wax (*Figure 10b*). At higher bulk wax concentrations the surface depletes in wax, linearly with the bulk wax concentration.

Static secondary-ion mass spectroscopy. Surface phase diagrams (*Figure 11*) have been prepared from s.s.i.m.s. data, assuming the same sensitivity factor for all blends. As in the case of X.p.s., the surface composition is presented as an excess quantity. The s.s.i.m.s. sensitivities were calculated from the experimental data of S50/PMMA and S58/PMMA blends assuming complete compatibility for the wax content not exceeding $\approx$8–9 monomer per cent (5 wt%), i.e. in the region where X.p.s. showed observed concentration = bulk concentration.

The results of s.s.i.m.s. investigations also distinguish two groups of surface behaviour. The character of observed changes in surface composition is mainly similar to that of the X.p.s. experiments. The X.p.s. and s.s.i.m.s. data change in the same way with blend composition for low-chlorine-content waxes (S42 and S48). However, the X.p.s. and s.s.i.m.s. compositions for the higher chlorinated waxes (S50 and S58)/PMMA systems are similar only up to $\approx$15 monomer per cent ($\approx$8–10 wt% for S50 and S58 respectively) of wax addition. Above this, s.s.i.m.s. detected a sudden depletion in the wax excess, which reduced with increasing wax concentration, contrary to the linear depletion obtained from X.p.s. (*Figure 10b*).

In regions where the X.p.s. and s.s.i.m.s. data behave in the same fashion, the absolute values of the wax excess or depletion on the surface calculated from X.p.s. spectra are lower than those calculated from s.s.i.m.s. ones.

Contact angles. Surface energies of the blends and their components were calculated from contact angle measurements. They have been compared to those calculated for the bulk composition[48], and are shown in *Figure 12*.

Because of the very similar values of the surface energies of the blend components, the differences detected are very small. It is worth noting that the blends again fall into two groups, namely S42(S48)/PMMA and S50(S58)/PMMA. Considering compositions up to 5 wt% ($\approx$7–11 monomer per cent for S58–S42 respectively), the experimental value for the surface energy, γ_S, is higher for blends prepared with S50 and S58 waxes, and lower for S42 or S48 chloroparaffins, then calculated additively for the bulk composition. In this way the contact angle data mirror the X.p.s. and s.s.i.m.s. results. Above 5 wt% of wax concentration, i.e. in the region of reduced compatibility, the expected

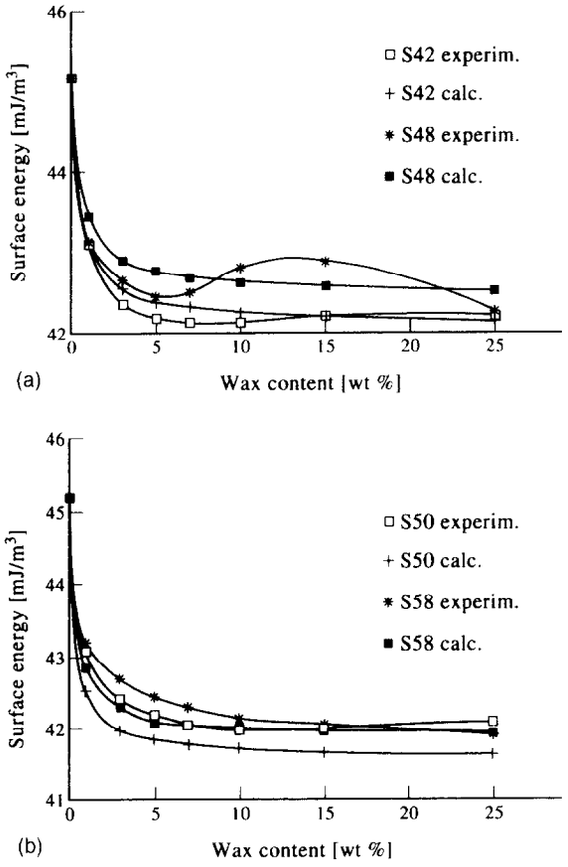

Figure 12 Surface energy γ_S of CPE wax/PMMA blends: (a) S42/PMMA and S48/PMMA, obtained experimentally and calculated from the bulk composition[48]; and (b) S50/PMMA and S58/PMMA obtained likewise

Table 6 Surface excess of wax in blend

Technique	CPE wax surface excess		Composition (wax monomer %)
	S42 and S48	S50 and S58	
X.p.s.	excess	zero	
S.s.i.m.s.	excess	zero	<10
Contact angle	excess	deficit	
X.p.s.	excess	deficit	>30
S.s.i.m.s.	excess	deficit	

changes in surface energy are minimal, and considering the experimental error and phase behaviour, the data are less readily interpreted.

Surface composition

The surface analysis techniques varied with respect to the depth of sample probed. The X.p.s. data are obtained from a typical depth of ca. 3 nm. S.s.i.m.s. is more surface-sensitive, and probes ca. 1 nm, whilst the contact angle determinations probably also probe depths of this order or less. It is instructive to compare the data across the surface techniques employed, and *Table 6* attempts to summarize and simplify the results of the surface analyses.

Considering first the blends with wax concentrations less than 10 monomer per cent, the low-chlorine waxes, S42 and S48, show a segregation of wax to the surface, by X.p.s., s.s.i.m.s. and contact angle. In a mixture, the component with lower surface energy may be expected to migrate to the surface in the absence of any specific constraints. The observed excess of wax at the surface may therefore be assumed to arise from a lowering of the overall surface energy.

In contrast, the high-chlorine waxes, S50 and S58, in the same bulk composition region, have similar surface and bulk concentrations according to X.p.s. The corresponding contact angle data suggest that there may even be a deficit of wax at the surface. These data can be reconciled, keeping in mind that the contact angle technique is more surface-sensitive, if there is a concentration gradient within ca. 3 nm from the surface. In theory, the s.s.i.m.s. data should verify the contact angle results. However, it was necessary to assume s.s.i.m.s. sensitivities to calculate the concentrations. The s.s.i.m.s. data were normalized by making the simplest assumption, i.e. that the X.p.s. results for these compositions indicated a homogeneous mixture with no surface segregation. It is possible, therefore, that the true surface compositions are slightly deficient in wax, and the s.s.i.m.s. sensitivities are not quite correct.

In this case, the s.s.i.m.s. data for S42 and S48 above would have to be revised, which would result in a decrease in the measured wax surface excess. Nevertheless, the trend would be unchanged, and noting the corresponding contact angle data, changes in composition would be minor and the surfaces would still have an excess of wax.

Turning now to the high bulk concentrations, greater than 20 monomer per cent, both X.p.s. and s.s.i.m.s. show that the low-chlorine S42 and S48 wax blends have an excess of wax at the surface. On the other hand, the high-chlorine S50 and S58 wax blends have a surface excess of PMMA.

The waxes fall, therefore, into two groups, low and high chlorine. The low-chlorine waxes form blends with a tendency for segregation of the wax *to* the surface, and the high-chlorine waxes form blends with *no* segregation of wax to the surface or migration of wax *from* the surface. These effects are most likely to result from the extent and nature of the specific interactions in the blends. The high-chlorine waxes interact with the host PMMA more than the low-chlorine waxes. The bulk specific interactions for the former overcome the surface free-energy contributions, and reduce the amount of wax at the surface.

The process is complex, depending also on the bulk composition of the blends, and will relate to the multiphase nature of the bulk system, described above.

CONCLUSIONS

Bulk investigations using d.e.t.a. and d.m.t.a. suggest a microheterogeneous structure for all systems. It has been shown by the n.m.r. and *FT*i.r. data that chlorine contents of a certain range lead to miscibility of chloroparaffin wax with PMMA. The dramatic effect of increasing the chlorine content from 42 to 58 wt% on the 'acidity' of the wax and its heat of mixing with PMMA is described.

Specific interactions have been revealed as a main factor deciding compatibility. These specific interactions are mainly the result of an attraction between the α-H from CPE wax and the carbonyl oxygen from PMMA.

Other possible attractive interactions seem to play a minor role.

The ratio of $CHCl/CH_2$ groups of the chloroparaffin can be used as a measure of its potential to form miscible blends with PMMA. Results obtained for the bulk miscibility of the system are in good agreement with the data presented by Tremblay and Prud'homme[23], who suggested a degree of chlorination of the polymer of 48–50 wt% to be indispensable in obtaining compatible blends with PMMA. Specific interactions existing in the CPE wax/PMMA systems were found to be very weak.

According to their molecular behaviour, the waxes fall into two groups, namely below 48–50 wt% and above 48–50 wt% of chlorine, in agreement with the results reported by Higgins *et al.*[2–4] for waxes of the type used in this study blended with oligomeric PMMA.

Surface compositions have the same division of behaviour as bulk ones. Blends show surface segregation dependent on the chlorine content in the waxes and the blend composition.

Though the chlorine contents of S48 and S50 do not greatly differ, the waxes do not behave similarly, and fall into different groups, noted above. The interaction of the S48 and S50 waxes in the blends, as measured by i.r. frequency shifts or intensity ratios, are similar and do not distinguish any possible traits, with the exception of the wax–pyridine experiments, which suggest that S50 is closer to S58 wax in potential for interactions. The greater basicity of pyridine, compared to PMMA, will facilitate the acid–base interactions, thus revealing the differences.

An important difference in S48 and S50 waxes is observed in the d.s.c. measurements. The lower-molecular-weight S50 wax has a lower T_g. The greater flexibility that this implies may be sufficient to move the S50 wax towards the more compatible behaviour.

The similar surface and bulk compositions, observed for the low wax content systems, is especially relevant from the blend compatibility point of view, CPE waxes being recommended plasticizers for PMMA. The evidence suggests that blends of S50 or S58 form the most miscible systems with PMMA at low wax contents, for wax concentrations $\leqslant 5$ wt% ($\approx$8–9 monomer per cent depending on the wax), whereas S42 and S48 are more incompatible. The degree of immiscibility influences the extent of surface segregation of the wax, which is pronounced with the waxes of low degree of chlorination.

ACKNOWLEDGEMENTS

Dariusz M. Bielinski thanks Strathclyde University for a studentship. We are grateful to ICI Chemicals & Polymers (Runcorn, UK) for donation of CPE waxes.

REFERENCES

1 Olabisi, O., Robeson, L. M. and Shaw, M. T. 'Polymer–Polymer Miscibility', Academic Press, New York, 1979, Ch. 5, p. 217
2 Walsh, D. J., Higgins, J. S. and Chai, Z. *Polymer* 1982, **23**, 336
3 Chai, Z., Sun, R., Walsh, D. J. and Higgins, J. S. *Polymer* 1983, **24**, 263
4 Clark, J. N., Fernandez, M. L., Tomlins, P. E. and Higgins, J. S. *Macromolecules* 1993, **26**, 5897
5 Corish, P. J. and Powell, B. D. W. *Rubber Chem. Technol.* 1974, **47**, 481
6 Vorenkamp, E. J. and Challa, G. *Polymer* 1988, **29**, 86
7 Lemieux, E., Prud'homme, R. E., Forte, R., Jerome, R. and Teyssie, P. *Macromolecules* 1988, **21**, 2148
8 Allard, D. E. and Prud'homme, R. E. *J. Appl. Polym. Sci.* 1982, **27**, 559
9 Vorenkamp, E. J., ten Brinke, G., Meijer, J. G., Jager, H. and Challa, G., *Polymer* 1985, **26**, 1725
10 Schurer, J. W., Boer, A. D. and Challa, G. *Polymer* 1975, **16**, 201
11 Zhao, J. and Prud'homme, R. E. *Macromolecules* 1990, **23**, 713
12 Short, R. D., Ameen, A. P., Jackson, S. T., Pawson, D. J., O'Toole, L. and Ward, A. J. *Vacuum* 1993, **44**, 1143
13 Hayward, D., Gawayne, M., Mahboubian-Jones, B. and Pethrick, R. A. *J. Phys. (E) Sci. Instrum.* 1984, **17**, 683
14 Briggs, D. and Seah, M. P. 'Practical Surface Analysis', 2nd Edn., Wiley, Chichester, 1992, Vol. 1
15 Fowkes, F. M. *Ind. Eng. Chem.* 1964, **56**, 40
16 Janczuk, B. and Bialopiotrowicz, T. *Polimery* 1987, **32**, 269
17 Tsutsumi, K. and Abe, Y. *Colloid Polym. Sci.* 1989, **267**, 637
18 Zaborski, M., Rucinski, J. and Bielinski, D. *Polimery* 1991, **3**, 109
19 Higgins, J. S., Fruitwala, H. A. and Tomlins, P. E. *Br. Polym. J.* 1989, **21**, 247
20 Varnell, D. F., Moskala, E. J., Painter, P. C. and Coleman, M. M. *Polym. Eng. Sci.* 1983, **23**, 658
21 Parmer, J. F., Dickinson, L. Ch., Chien, J. C. W. and Porter, R. S. *Macromolecules* 1989, **22**, 1078
22 Fowkes, F. M., Tischler, D. O., Wolfe, J. A., Lannigan, L. A., Ademu-John, C. A. and Halliwell, M. J. *J. Polym. Sci., Polym. Chem. Edn.* 1984, **22**, 547
23 Tremblay, C. and Prud'homme, R. E. *J. Polym. Sci., Polym. Phys. Edn.* 1984, **22**, 1857
24 White, A. J. and Flisko, F. E. *J. Polym. Sci., Polym. Lett. Edn.* 1982, **20**, 525
25 Bovey, F. A. and Tiers, G. V. D. *J. Polym. Sci.* 1960, **44**, 173
26 Zhou, Z., Dai, Y., Tian, W., Wu, S., Jing, F. and Feng, Z. *Sci. China (B)* 1992, **35**, 769
27 Komoroski, R. A., Parker, G. and Shockcor, J. P. *Macromolecules* 1985, **18**, 1257
28 Komoroski, R. A., Parker, G. and Lehr, M. H. *Macromolecules* 1982, **15**, 844
29 Keller, F. *Faserforsch. Textiltech.* 1978, **29**, 490
30 Keller, F. *Plaste Kautsch.* 1976, **23**, 730
31 Keller, F. and Magge, C. *Plaste Kautsch.* 1977, **24**, 88
32 Hill, R. G., Tomlins, P. E. and Higgins, J. S. *Macromolecules* 1985, **18**, 2555
33 Cesteros, L. C., Isasi, J. R. and Katime, I. *J. Polym. Sci., Polym. Phys. Edn.* 1994, **32**, 223
34 Klinsberger, E. (Ed.) 'Pyridine and its Derivatives, Part I', Interscience, New York, 1960, p. 11
35 Fowkes, F. M. in 'Acid–Base Interactions' (Eds K. L. Mittal and H. R. Anderson), VSP, The Netherlands, 1991, p. 93
36 Garton, A., Aubin, M. and Prud'homme, R. E. *J. Polym. Sci., Polym. Lett. Edn.* 1983, **21**, 45
37 Ma, D.-Z. and Prud'homme, R. E. *Polymer* 1990, **31**, 917
38 Walsh, D. J. and Rostani, S. *Adv. Polym. Sci.* 1985, **70**, 119
39 Simha, R. and Boyer, R. F. *J. Chem. Phys.* 1962, **37**, 1003
40 Perrin, P. and Prud'homme, R. E. *Polymer* 1991, **32**, 1468
41 Kögler, G. and Mirau, P. A. *Polymer* 1992, **25**, 598
42 Sofue, S. and Tamura, N. *J. Appl. Polym. Sci.: Polym. Symp.* 1993, **52**, 261
43 ten Brinke, G., Karasz, F. E. and MacKnight, W. J. *Macromolecules* 1983, **16**, 1827
44 Fried, J. R., Karasz, F. E. and MacKnight, W. J. in 'Polymer Blends' (Eds D. R. Paul and S. Newman), Academic Press, New York, 1978
45 Kaplan, D. S. *J. Appl. Polym. Sci.* 1976, **20**, 2616
46 Hemsley, D. A. 'The Light Microscopy of Synthetic Polymers', Oxford University Press, New York, 1984
47 Fox, T. G. *Bull. Am. Phys. Soc.* 1956, **1**, 123
48 Wu, S. 'Polymer Interface and Adhesion', Marcel Dekker, New York, 1982, Ch. 3, p. 79